Comparative Analysis of Different Plasma Gases and Their Effects on Cutting Performance in High-Strength Alloys

Roopam Mittal, Saurabh Tege, Deepak Paliwal, Surbhi Mishra,
Department of Mechanical Engineering, Geetanjali Institute of Technical Studies, India,

ABSTRACT

The increasing use of high-strength alloys, such as Sailhard steel, Abrex 400, and 304 L stainless steel, in structural applications has increased the need for efficient cutting methods. Plasma arc cutting (PAC) is a versatile technique; however, the impact of plasma gases on the cut quality and efficiency is not fully understood. This study examined the effects of four gases (air, oxygen, nitrogen, and argon) at various flow rates using a full factorial design. This study evaluated the material removal rate (MRR), kerf width, surface roughness, and dross formation. The study revealed that gas type was the most critical factor ($p < 0.001$). Oxygen yielded the highest MRR, averaging 145.2 mm^3/min, but resulted in the widest kerf (2.18 mm) and most dross (8.0 mg/cm). Argon achieved the narrowest kerf (1.53 mm) and smoothest surface (Ra = 2.23 μm). Nitrogen balanced productivity and quality, with moderate MRR (118.6 mm^3/min) and least dross (3.8 mg/cm). Air exhibited intermediate performance across the metrics. Increasing the flow rate reduced the dross but widened the kerf in oxygen-assisted cutting. It has been identified that oxygen is the most effective for productivity, argon excels in precision and surface finish, and nitrogen reduces post-processing needs. These insights offer clear guidelines for selecting plasma gases for the industrial cutting of high-strength alloys.

Key words: Plasma Arc Cutting (PAC), High-Strength Alloys, Material Removal Rate (MRR), Kerf Width, Surface Roughness (Ra), Dross Formation

1. Introduction

High-strength alloys are essential in engineering fields owing to their distinctive characteristics, such as high strength-to-weight ratios, superior mechanical performance, and resistance to environmental damage. These alloys are utilized across industries, including aerospace, oil and gas, and nuclear engineering, offering benefits over conventional materials. In the aerospace sector, lightweight yet durable materials are crucial for achieving both safety and performance. Among these, advanced aluminum alloys play a vital role, offering the strength required for rockets, aircraft, and spacecraft while keeping the overall weight minimal to enhance flight efficiency. Alloys belonging to the Al-Cu-Mg and Al-Zn-Mg-Cu families are particularly recognized for their superior mechanical properties, making them highly suitable for demanding structural applications (Speidel & Hyatt, 1972). High-Entropy Alloys (HEAs), exemplified by the CoCrFeNiMn composition, are gaining importance for structural use due to their ability to combine high strength with good ductility. Their inherent phase stability and reliable performance, even under cryogenic conditions, make them highly attractive compared to conventional alloys. Recent progress in fabrication routes, including powder metallurgy, has further enhanced their microstructural integrity and mechanical behavior, expanding their suitability for challenging operating environments (Nagarjuna et al., 2025; Shahmir et al., 2023). Nanostructured materials with high strength, particularly those derived from aluminum, have been engineered for situations in the Oil and Gas sector where minimizing weight and ensuring dependability are crucial. These

advanced materials exhibit exceptional specific strength, often surpassing that of conventional steels. Moreover, by tailoring their microstructure, their properties can be adapted for specialized requirements, such as enhanced resistance to dynamic loading and corrosive environments (Zhang et al., 2012). High-Entropy Alloys (HEAs) are increasingly being explored for nuclear applications owing to their ability to withstand radiation damage while retaining strong mechanical performance. Recent developments have focused on Ni- and Co-free systems, specifically designed to operate under extreme reactor environments. These alloys exhibit high melting temperatures along with superior durability, making them promising candidates for advanced nuclear technologies (Wakai et al., 2023). The development of metastable aluminum-based alloys through advanced quenching techniques has resulted in materials that exhibit remarkable tensile strength and enhanced thermal resistance. Compared to conventional crystalline alloys, these materials demonstrate superior mechanical performance, which has encouraged their adoption across diverse fields, including industrial machinery, structural components, and sporting equipment (Inoue et al., 2015). Titanium alloys are highly valued in biomedical engineering due to their excellent biocompatibility and resistance to corrosion, qualities that make them particularly suitable for medical implants and related applications. Among them, Ti-6Al-4V stands out for its impressive strength-to-weight ratio, which supports its widespread use in critical healthcare solutions (H.A. Besisa & Yajima, 2024). Engineering applications increasingly rely on high-strength alloys because of their specialized properties that align with diverse industrial requirements. Progress in alloy design is paving the way for further improvements in service life, operational effectiveness, and technological advancement across different fields (Darolia et al., 1992; Wakai et al., 2023).

Plasma gases significantly influence the performance of Plasma Arc Cutting systems by affecting process efficiency, cutting speed, and the quality of the finished surface. These systems employ gases like oxygen, nitrogen, and argon, either individually or in combination, each contributing differently to energy transfer. Oxygen accelerates steel cutting through oxidation reactions, while argon allows precise cutting but with slower progress (Girard et al., 2006). The application of suitable gas pressure is critical in Plasma Arc Cutting, as it facilitates the removal of molten metal, reduces dross accumulation, and enhances the smoothness of the cut surface. Experimental investigations using Taguchi-based optimization confirm that proper adjustment of gas pressure leads to reduced surface roughness and narrower kerf widths, thereby improving overall cut quality (Adalarasan et al., 2015; Ramakrishnan et al., 2018). The chemical composition of the plasma gas directly influences the plasma jet's temperature and electron density, both of which are critical parameters for efficient material cutting. Employing oxygen-based plasma with carefully regulated composition and flow conditions can significantly increase thermal energy and improve cutting efficiency. Introducing nitrogen into the plasma jet can alter the shock wave dynamics and the entrainment of air, thereby affecting the cutting process (Girard et al., 2006). Selecting the correct plasma gas is essential to ensure compatibility with the material being cut. For commercial-grade aluminum, optimizing gas pressure has been shown to enhance cutting precision, highlighting the importance of tailoring gas parameters for specific materials (Choudhury et al., 2024). Nitrogen-based gas curtains serve to protect the plasma jet from environmental interference, influence plasma chemistry, minimize oxidative reactions, and mitigate thermal impact during cutting operations (Bekeschus et al., 2015). The performance and quality of plasma cutting are strongly dependent on gas selection. Adjusting gas type, pressure, and flow enables industries to achieve precise cuts and optimize operational efficiency.

A comparative study of plasma gases is essential due to the wide range of applications of plasma technology, spanning areas such as medicine and environmental science. Understanding the differences among plasma gases is important because each type can uniquely influence chemical reactions and biological processes. Cold plasmas, a type of ionized gas used in plasma medicine, generate reactive species that modulate biological functions and have applications in both healing and cancer treatment. To advance these therapies, it is important to study the specific impacts of various gases on plasma-treated cells, enabling the development of optimized medical practices (Bekeschus et al., 2017). Plasma gases are applied in dermatology for their ability to interact with tissues, enabling targeted therapeutic effects and necessitating careful consideration of each gas's properties to customize treatments effectively (Friedman, 2020). In parallel, industrial applications use plasma gases to manage greenhouse emissions, breaking down harmful compounds and contributing to environmental sustainability (Indarto et al., 2008). In agriculture and food safety, plasma gases are employed to produce plasma-activated water (PAW), which can improve crop yield and enhance the safety of food products. The performance of PAW systems depends on the characteristics of the plasma gas used, highlighting the importance of comparative studies to optimize system design (Misra et al., 2024). Comparing plasma gases is crucial for optimizing their performance in diverse applications. Insight into their characteristics and behaviors enables improvements in operational efficiency and safety across medical, environmental, and industrial domains.

The evolution of fiber laser cutting technology reflects a trend in the industry toward achieving greater accuracy in cutting operations (Madić et al., 2024).These innovations are crucial for plasma cutting, where precise cuts with minimal waste are essential. Experimental methods, such as the one-factor-at-a-time (OFAT) approach, help optimize parameter settings, improving cut efficiency and quality (Madić et al., 2024). Such techniques are applied to plasma cutting, where the gas flow rate, nozzle design, and current settings influence the results. Understanding cutting friction behavior can extend tool life and enhance surface quality, which are critical aspects of advanced cutting processes (Liang et al., 2022). Although discussed for abrasive water jet cutting, micro- and nanomachining principles are increasingly relevant to plasma cutting, allowing finer details and complex geometries needed in precision industries (S Alsoufi, 2017). Modern cutting technologies aim to minimize waste and energy consumption, which is a significant trend in plasma cutting. Industries can achieve more sustainable operations by refining methods and equipment design. The current state of plasma cutting reflects innovations in precision, efficiency, and sustainability, similar to other cutting technologies.

Although plasma arc cutting (PAC) has been extensively studied, most existing studies focus on optimizing single process parameters, such as gas flow rate, current, or nozzle design, in isolation. Oxygen, nitrogen, and argon have been individually examined for their roles in influencing kerf quality, surface roughness, and dross formation; there is limited comparative research that systematically analyzes their combined effects across different high-strength alloys. The lack of integrated studies that correlate plasma gas composition, pressure, and flow rate with both performance metrics (cutting speed, efficiency, and accuracy) and sustainability indicators (energy use and waste reduction) leaves a significant knowledge gap. This gap restricts the development of predictive models and generalized guidelines that industries can adopt for cost-effective and high-precision cutting of diverse high-strength materials. This study addresses this gap by utilizing four distinct plasma gases: air, oxygen, nitrogen, and argon, and examines their impact on key performance indicators when cutting Sailhard steel, Abrex 400, and 304 L stainless steel.

2. Experimental Methodology

2. 1 Description of plasma cutting equipment used

A CNC portable plasma arc cutting system was used for the experiments. The system was equipped with a high-frequency inverter-based power supply that could operate within a current range of 40-200 A. A water-cooled cutting torch was used in the experiments. The cutting torch had a nozzle orifice with a diameter of 1.2 mm. The torch movement was controlled using CNC software, which ensured accurate cutting paths and kerf geometry. The gas flow was regulated between 20-40 L/min using precision flow meters. A stand-off distance of 2 mm was maintained to minimize the arc instability. The experimental setup enabled precise manipulation of the cutting conditions, permitting systematic variation of plasma gas composition and flow while maintaining other parameters unchanged.

2. 2 Specifications of high-strength alloy samples

As summarized in Table 1, the study used three different high-strength alloy samples, each chosen to represent structural, wear-resistant, or corrosion-resistant types. Sailhard Steel featured a thickness of 8 mm, hardness between 200 and 220 HB, and a tensile strength of 750 MPa. Abrex 400 Steel, measuring 10 mm in thickness, had the highest hardness (360–400 HB) and tensile strength (1200 MPa) of all samples. The 304 L Stainless Steel, the thinnest at 6 mm, displayed a hardness of 150 HB and tensile strength of 520 MPa. All three alloy samples were shaped into 150 mm × 150 mm plates. Prior to testing, the plates were meticulously cleaned to remove rust and other surface residues, guaranteeing consistent experimental conditions. By selecting these alloys, the study encompassed a range of material characteristics, allowing evaluation of plasma gas performance under different conditions of hardness, thickness, and strength.

Table 1. Properties of High-Strength Alloy Samples

Alloy Type	Thickness (mm)	Hardness (HB)	Tensile Strength (MPa)	Plate Size (mm)
Sailhard Steel	8	200–220	750	150 × 150
Abrex 400 Steel	10	360–400	1200	150 × 150
304L Stainless Steel	6	150	520	150 × 150

2. 3 Control variables and parameters

The experiment incorporated both fixed and variable parameters to methodically examine the influence of plasma gas on cutting performance, as summarized in Table 2. Fixed parameters were maintained to isolate the effects of variable parameters, such as gas type and flow rate, on the cutting outcomes. This strategy allows researchers to analyze the influence of different gases and flow rates on cutting performance more effectively, limiting the contribution of other parameters. The choice of air, oxygen, nitrogen, and argon was guided by their relevance in industrial applications and their anticipated effects on cut quality. Air was chosen due to its cost-effectiveness and easy availability. Oxygen was selected for its capacity to facilitate exothermic oxidation, which can increase the material removal rate. Nitrogen was employed for its inert properties, helping to minimize oxidation and produce cleaner cuts. The choice of argon was motivated by its ability to produce consistent arcs and improve surface smoothness, despite reduced cutting speed. A flow rate between 20 and 40 L/min was selected to provide a realistic operating range that could influence cut quality without destabilizing the plasma arc.

By varying these parameters, the researchers could comprehensively assess how different gas types and flow rates affect key performance indicators, such as the material removal rate, kerf width, surface roughness, and dross formation, across different high-strength alloys.

Table 2. Control and Variable Parameters

Parameter	Value/Levels	Type
Cutting Current	120 A	Fixed
Arc Voltage	140 V	Fixed
Stand-off Distance	2 mm	Fixed
Nozzle Diameter	1.2 mm	Fixed
Cutting Speed	1000 mm/min	Fixed
Plasma Gas Type	Air, Oxygen, Nitrogen, Argon	Variable
Gas Flow Rate	20, 30, 40 L/min	Variable

2. 4 Factorial design of experiments

A full factorial design was employed for the experiments, allowing for a comprehensive examination of all possible combinations of the factors being studied. The experiment considered three main factors: four types of plasma gases, three levels of gas flow rates, and three types of alloys as shown in Table 3. The combination of these factors resulted in 36 unique treatments (four gases × three flow rates × three alloys = 36). The experimental design included two repetitions per treatment, totaling 72 runs. Plasma gases were denoted G1 through G4 for Air, Oxygen, Nitrogen, and Argon. Three gas flow levels, 20, 30, and 40 L/min, were coded F1–F3, and the three alloy types—Sailhard, Abrex 400, and 304L Stainless Steel—were represented as M1–M3.

The factorial approach facilitated a systematic investigation of the individual and combined effects of plasma gas type, flow rate, and alloy type. Testing every possible combination allowed the researchers to analyze their influence on cutting performance across diverse conditions. The resulting dataset supports robust statistical evaluation, highlighting significant factors and their relative impact on the cutting process.

Table 3. Factor, Level and Notation for Analysis

Factor	Levels	Notation
Plasma Gas Type	Air, Oxygen, Nitrogen, Argon	G1–G4
Gas Flow Rate (L/min)	20, 30, 40	F1–F3
Alloy Type	Sailhard, Abrex 400, 304L Stainless	M1–M3

3. Results and Analysis

3. 1 ANOVA results for Material Removal Rate

The ANOVA results for Material Removal Rate (MRR) in the plasma arc cutting study, summarized in Table 4, indicated several key insights. Plasma gas type emerged as the most influential factor, with a p-value below 0.001, accounting for roughly 72% of the variance in MRR (partial $\eta^2 \approx 0.72$). The material type also significantly influenced the Material Removal Rate (MRR). A notable interaction between plasma gas type and material was observed. Oxygen consistently resulted in the highest MRR across all alloys, likely due to the exothermic oxidation reactions that contribute additional chemical energy to the cutting arc. Nitrogen achieved the

second-highest MRR, while air yielded moderate removal rates. Argon produced the lowest MRR values, which can be attributed to its high ionization potential and chemically inert behavior.

Table 4. ANOVA for MRR

Source	F-value	p-value	Partial η^2
Gas	85.3	<0.001	0.72
Flow	4.9	0.015	0.08
Material	10.1	<0.001	0.12
Gas × Material	6.2	0.002	0.10

The F-value for the plasma gas factor was 85.3, far exceeding the F-values of other factors, highlighting its dominant effect on MRR. While less influential than gas type, the gas flow rate showed a modest but statistically significant impact on MRR ($p = 0.015$, partial $\eta^2 = 0.08$). These ANOVA results underscore the critical role of plasma gas selection in achieving optimal MRR during plasma arc cutting of high-strength alloys, with oxygen showing the greatest effectiveness. The Gas × Material interaction plot illustrates the influence of different gases on MRR across the tested materials. The plot illustrates a notable interaction between plasma gas type and the material being cut, influencing MRR. This aligns with the ANOVA findings, which identified the Gas × Material interaction as significant. Oxygen, in particular, markedly increased MRR, especially when applied to 304 L stainless steel. This finding is consistent with the general observation that oxygen consistently provides the highest MRR across all alloys.

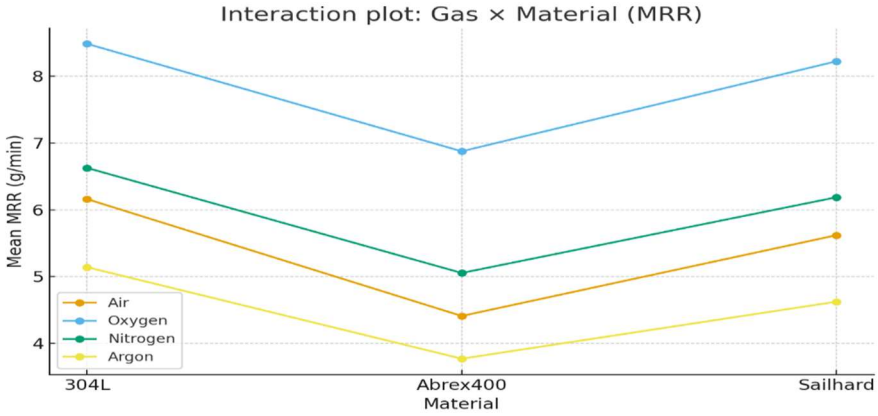

Figure 1: High Strength Material Vs Mean MRR (Interaction Plot)

The Figure 1 indicates that argon consistently underperformed for all materials in terms of MRR. This aligns with the earlier statement that argon exhibited the lowest MRR values. The plot illustrates how different gases perform differently on various materials. For instance, it may demonstrate that the MRR advantage of oxygen is more pronounced for certain alloys than for others. The plot visually represents the relative performance of different gases (oxygen, nitrogen, air, and argon) for each material type, allowing for easy comparison.

3.2 ANOVA Results for Kerf Width

Researchers analyzed the kerf width as part of their study on the plasma arc cutting of high-strength alloys as presented in Table 5 and 6. Analysis of variance (ANOVA) showed that both gas type

and material type were significant factors affecting the kerf width ($p < 0.01$). A small yet noticeable effect of the flow rate on cutting performance was observed.

Table 5: ANOVA for Kerf Width

Source	F-value	p-value	Partial η^2
Gas	42.7	<0.001	0.61
Flow	3.5	0.038	0.07
Material	8.2	0.001	0.11
Gas × Flow	5.1	0.004	0.09
Error	–	–	–
Total	–	–	–

Table 6. Summary of Kerf Width by Gas

Gas	Mean Kerf (mm)	Std Dev
Oxygen	2.18	0.12
Air	2.01	0.09
Nitrogen	1.82	0.08
Argon	1.53	0.07

The widest kerf, roughly 2.18 mm, was observed with oxygen, which can be attributed to strong exothermic reactions and increased material removal. Argon produced the narrowest kerf at about 1.5 mm, reflecting its stable and relatively cooler arc. Kerf widths for nitrogen and air were intermediate.

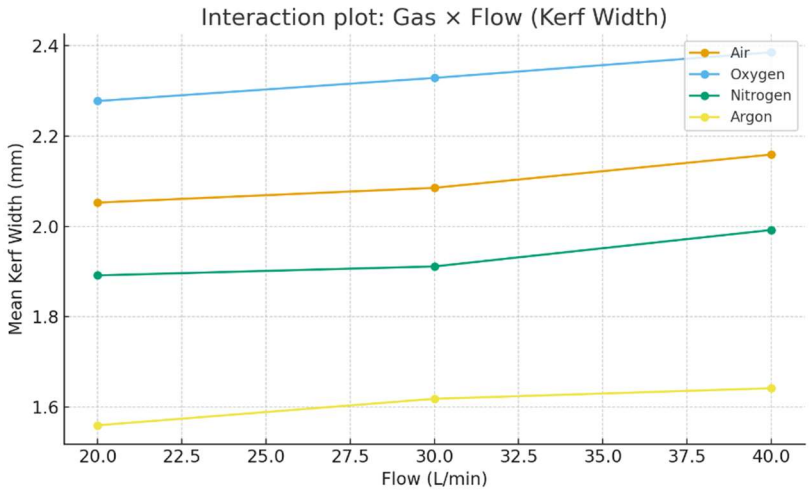

Figure 2: Gas Flow Vs Mean Kerf Width (Interaction Plot)

The study also explored the interaction between gas type and flow rate on kerf width. For oxygen, the kerf width tended to increase at higher flow rates, while argon exhibited relatively stable kerf widths across the tested flow range. This analysis offers valuable insights into the impact of different plasma gases on kerf width, which is essential for controlling dimensional accuracy and minimizing material waste in plasma arc cutting.

Figure 2 illustrates the interaction between plasma gas type and flow rate and its effect on kerf width. This interaction is significant and noteworthy. The plot indicates that using oxygen as the plasma gas results in an increase in kerf width as the flow rate rises. The results suggest that higher flow rates of oxygen cause an expansion in kerf width. Conversely, argon produced kerf widths

that were largely unaffected by changes in flow rate. The data indicate that argon maintains uniform kerf widths despite changes in flow rate.

The plot provides a comparison of how oxygen, argon, nitrogen, and air perform in terms of kerf width at different flow rates. The plot provided a clear visual comparison of the kerf width behavior of each gas as flow rates varied. Argon's stability across flow rates supports earlier findings that highlight its effectiveness for precision applications. The plot provides useful insights for optimizing the cutting process, illustrating how varying the flow rate for different gases affects kerf width—a key factor in achieving precise cuts and maintaining dimensional accuracy.

3.3 ANOVA Results for Surface Roughness and Dross Formation

The ANOVA results for Surface Roughness and Dross Formation, presented in Tables 7 and 8, provided important insights into how different factors influence these key quality parameters in plasma arc cutting.

For Surface Roughness (Ra), the type of plasma gas was the most influential factor ($p < 0.001$, $\eta^2 \approx 0.65$), while the material type also had a significant, though lesser, effect. Argon consistently produced the smoothest surfaces, with Ra values around 2.2 μm. Nitrogen resulted in moderately smooth finishes (Ra ≈ 2.8 μm). Air and Oxygen produced rougher surfaces (Ra ≈ 3.1-3.6 μm). These results are consistent with those of other studies have reportedrting smoother cut surfaces when using inert gases. The smoother finish achieved with argon is particularly advantageous in precision industries, such as aerospace and medical device fabrication.

In contrast, Dross Formation analysis revealed that the gas type was the most significant factor ($p < 0.001$, $\eta^2 \approx 0.68$). The flow rate also plays a major role in dross formation. Nitrogen produced the least amount of dross (≈ 3.8 mg/cm). Argon generated moderate dross (≈ 5.5 mg/cm). Air produced more dross (≈ 6.2 mg/cm) than argon. Oxygen led to the highest dross formation (≈ 8 mg/cm). Increasing the flow rate reduced the dross for all gases. The superior performance of nitrogen in reducing dross is consistent with other studies, highlighting its effectiveness in minimizing molten metal attachment. The results demonstrate a trade-off between productivity (higher with oxygen) and cut cleanliness (better with nitrogen and argon). These ANOVA results provide valuable insights for optimizing plasma cutting parameters based on the specific requirements of surface finish and dross minimization for different applications.

The Gas × material (Surface Roughness) and gas × flow (dross) Figure 3 provides valuable insights into the effects of different plasma gases on the surface quality and dross formation during plasma arc cutting. The Gas × Material (Surface Roughness) plot shows how different gases affect the surface finish across various materials. Argon consistently produced the smoothest surface across all the tested alloys. This indicates that argon is the best choice for applications requiring a high-quality surface finish. Nitrogen provided a good surface finish, particularly for stainless steel (likely 304 L). This suggests that nitrogen can be a good alternative to argon, especially for cutting stainless steel. Oxygen and air likely produced rougher surfaces than argon and nitrogen. The Gas × Flow (Dross) plot illustrates how dross formation is affected by both the gas type and flow rate. Higher flow rates generally reduced dross formation for all the gases. This indicates that increasing the gas flow can be a strategy to minimize dross, regardless of the gas used. Nitrogen exhibited the best performance in minimizing dross formation. This aligns with the ANOVA results showing that nitrogen produced the least dross (≈ 3.8 mg/cm).

Table 7. ANOVA for Surface Roughness and Dross Formation

Result for Surface Roughness (Ra)				Result for Dross Formation			
Source	**F-value**	**p-value**	**Partial η²**	**Source**	**F-value**	**p-value**	**Partial η²**
Gas	56.9	<0.001	0.65	Gas	63.4	<0.001	0.68
Flow	2.7	0.068	0.05	Flow	7.9	0.001	0.11
Material	6.8	0.002	0.10	Material	4.2	0.010	0.07
Gas × Material	4.3	0.009	0.08	Gas × Material	5.7	0.003	0.09
Error	–	–	–	Error	-	-	-
Total	–	–	–	Total	-	-	-

Table 8. Mean Ra and Dross Formation by Gas

Gas	Mean Ra (µm)	Std Dev	Gas	Mean Ra (µm)	Std Dev
Argon	2.23	0.18	Argon	5.5	0.3
Nitrogen	2.82	0.22	Nitrogen	3.8	0.3
Air	3.09	0.24	Air	6.2	0.4
Oxygen	3.61	0.29	Oxygen	8.0	0.5

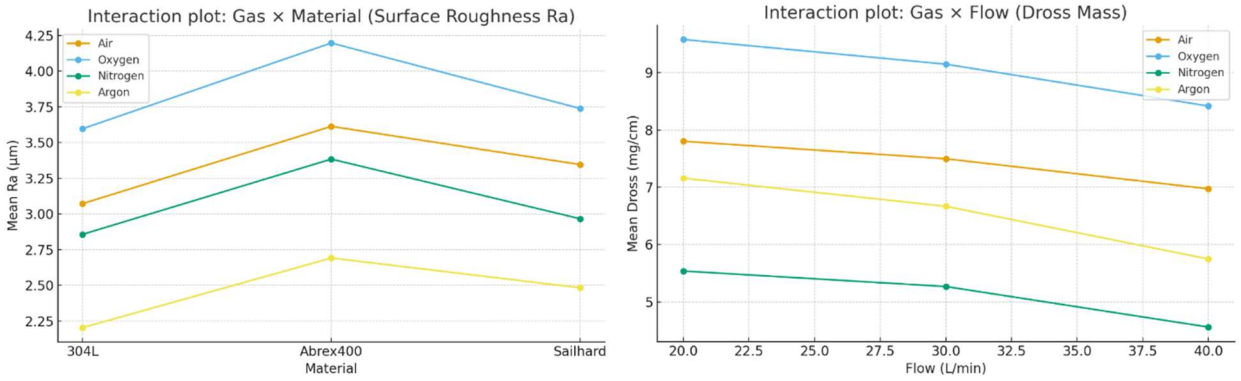

Figure 3: High Strength Material Vs Mean Surface Finish Vs Mean Dross (Interaction Plot)

Comparing these plots reveals that different gases have distinct effects on surface roughness and dross formation. For example, argon provides the best surface finish, whereas nitrogen is more effective at minimizing dross. Analyzing this comparison helps to understand the balance between achieving a smooth surface and minimizing dross. The Surface Roughness plot suggests that gas performance differs with material type, underlining the importance of material considerations when selecting a plasma gas. These plots collectively suggest that optimizing gas type along with flow rate can significantly improve cut quality. They provide practical guidance for selecting the most suitable combination of gas and flow rate based on specific objectives, such as achieving smoother surfaces or reducing dross, and on the material being cut. Together, these plots provide a detailed view of how gas type, flow rate, and material interact to influence key cut quality factors: surface roughness and dross formation. This information is essential for optimizing plasma cutting processes across a range of industrial applications.

4. Conclusion

The study highlighted the significant impact of plasma gas type on the performance of plasma arc cutting in high-strength alloys. Among the four gases tested, oxygen achieved the highest material removal rate (≈145 mm^3/min), indicating its suitability for applications where maximizing productivity is the main objective. However, this higher material removal rate came with trade-offs, including a wider kerf (≈2.18 mm), a rougher surface finish (Ra ≈ 3.61 μm), and the greatest dross formation (≈8.0 mg/cm).

Argon, on the other hand, consistently produced the narrowest kerf of approximately 1.53 mm and the finest surfaces (Ra ≈ 2.23 μm), despite a lower MRR of around 88 mm^3/min. Its characteristics make it suitable for tasks that prioritize accuracy and reduced finishing work. Nitrogen demonstrated a balanced performance, with a moderate material removal rate (≈118.6 mm^3/min) and the lowest dross accumulation (≈3.8 mg/cm), making it suitable for stainless steel and wear-resistant applications that require high edge quality. Air, on the other hand, delivered intermediate results and stood out primarily for its cost-effectiveness.

This study emphasizes that no single plasma gas excels across all performance measures. Instead, the choice of gas should be dictated by industrial priorities: oxygen for high throughput, argon for precision, nitrogen for cleaner edges, and air for economical cutting. These findings provide a practical framework for industries to align gas selection with specific performance and cost requirements for cutting high-strength alloys.

5. References

1. Adalarasan, R., Rajmohan, M., & Santhanakumar, M. (2015). Application of Grey Taguchi-based response surface methodology (GT-RSM) for optimizing the plasma arc cutting parameters of 304L stainless steel. *The International Journal of Advanced Manufacturing Technology, 78*(5–8), 1161–1170. https://doi.org/10.1007/s00170-014-6744-0
2. Bekeschus, S., Iseni, S., Reuter, S., Weltmann, K.-D., & Masur, K. (2015). Nitrogen Shielding of an Argon Plasma Jet and Its Effects on Human Immune Cells. *IEEE Transactions on Plasma Science, 43*(3), 776–781. https://doi.org/10.1109/tps.2015.2393379
3. Bekeschus, S., Schmidt, A., Niessner, F., Gerling, T., Weltmann, K.-D., & Wende, K. (2017). Basic Research in Plasma Medicine - A Throughput Approach from Liquids to Cells. *Journal of Visualized Experiments, 129*. https://doi.org/10.3791/56331-v
4. Choudhury, M. R., Saxena, K. K., Borah, A., Bhavani, B., Dutta, H., & Deka, U. (2024). Optimization of process parameters in plasma arc cutting of commercial-grade aluminium plate. *High Temperature Materials and Processes, 43*(1). https://doi.org/10.1515/htmp-2022-0329
5. Darolia, R., Konitzer, D. G., Field, R. D., Dobbs, J. R., Goldman, E. H., Chang, K. M., & Lahrman, D. F. (1992). Overview of NiAl Alloys for High Temperature Structural Applications (pp. 679–698). Springer Netherlands. https://doi.org/10.1007/978-94-011-2534-5_43
6. Friedman, P. C. (2020). Cold atmospheric pressure (physical) plasma in dermatology: where are we today? *International Journal of Dermatology, 59*(10), 1171–1184. https://doi.org/10.1111/ijd.15110
7. Girard, L., Razafinimanana, M., Teulet, P., Richard, F., Camy-Peyret, F., Baillot, E., & Gleizes, A. (2006). Experimental study of an oxygen plasma cutting torch: I. Spectroscopic analysis of the plasma jet. *Journal of Physics D: Applied Physics, 39*(8), 1543–1556. https://doi.org/10.1088/0022-3727/39/8/014
8. H.A Besisa, N., & Yajima, T. (2024). Titanium-Based Alloys: Classification and Diverse Applications. *Intechopen*. https://doi.org/10.5772/intechopen.1005269

9. Indarto, A., Song, H. K., Choi, J.-W., & Lee, H. (2008). Decomposition of greenhouse gases by plasma. *Environmental Chemistry Letters, 6*(4), 215–222. https://doi.org/10.1007/s10311-008-0160-3
10. Inoue, A., Zhu, S., Al-Marzouki, F., Liu, C. T., & Kong, F. (2015). Development and Applications of Highly Functional Al-based Materials by Use of Metastable Phases. *Materials Research, 18*(6), 1414–1425. https://doi.org/10.1590/1516-1439.058815
11. Liang, X., Cheung, C. F., Wang, C., Liu, Z., & Wang, B. (2022). Friction behaviors in the metal cutting process: state of the art and future perspectives. *International Journal of Extreme Manufacturing, 5*(1), 012002. https://doi.org/10.1088/2631-7990/ac9e27
12. Madić, M., Janković, P., & Jovanović, D. (2024). Fiber Laser Cutting Technology: Pilot Case Study in Mild Steel Cutting. *Spectrum of Mechanical Engineering and Operational Research, 1*(1), 1–9. https://doi.org/10.31181/smeor1120241
13. Misra, N. N., Naladala, T., & Alzahrani, K. J. (2024). Design of systems for plasma activated water (PAW) for agri-food applications. *Journal of Physics D: Applied Physics, 57*(49), 493003. https://doi.org/10.1088/1361-6463/ad77de
14. Nagarjuna, C., Dewangan, S. K., Rao, K. R., Ahn, B., Lee, H., & Song, E. (2025). A Review of Recent Developments in CoCrFeMnNi High-Entropy Alloys Processed by Powder Metallurgy. *Journal of Powder Materials, 32*(2), 144–163. https://doi.org/10.4150/jpm.2024.00430
15. Ramakrishnan, H., Karthikeyan, N., Ganesh, N., & Balasundaram, R. (2018). Experimental investigation of cut quality characteristics on SS321 using plasma arc cutting. *Journal of the Brazilian Society of Mechanical Sciences and Engineering, 40*(2). https://doi.org/10.1007/s40430-018-0997-8
16. S Alsoufi, M. (2017). State-of-the-Art in Abrasive Water Jet Cutting Technology and the Promise for Micro- and Nano-Machining. *International Journal of Mechanical Engineering and Applications, 5*(1), 1. https://doi.org/10.11648/j.ijmea.20170501.11
17. Shahmir, H., Mehranpour, M. S., Arsalan Shams, S. A., & Langdon, T. G. (2023). Twenty years of the CoCrFeNiMn high-entropy alloy: achieving exceptional mechanical properties through microstructure engineering. *Journal of Materials Research and Technology, 23*, 3362–3423. https://doi.org/10.1016/j.jmrt.2023.01.181
18. Speidel, M. O., & Hyatt, M. V. (1972). Stress-Corrosion Cracking of High-Strength Aluminum Alloys (pp. 115–335). Springer US. https://doi.org/10.1007/978-1-4615-8255-7_3
19. Wakai, E., Noto, H., Shibayama, T., Furuya, K., Wakui, T., Ando, M., Makimura, S., & Ishida, T. (2023). Recent improvement and evaluation of radiation resistance and magnetic properties of high entropy alloys and their applications. *Science Talks, 8*, 100278. https://doi.org/10.1016/j.sctalk.2023.100278
20. Zhang, Z., Salinas, B., & Xu, Z. (2012, June 12). High Strength Nanostructured Materials and Their Oil Field Applications. https://doi.org/10.2118/157092-ms